RSC Advances

Volume 1 | Number 1 | Jan 2013 | Pages 1–100

RSC Advances

www.rsc.org/advances

www.rsc.org/advances

ROYAL SOCIETY OF CHEMISTRY

RSC Advances

ARTICLE

Low-temperature catalytic oxidation of vinyl chloride over Ru modified Co_3O_4 catalysts

Chao Wang[a,b], Chuanhui Zhang[a,b], Wenchao Hua[a], Yanglong Guo[a,*], Guanzhong Lu[a], Sonia Gil[b], Anne Giroir-Fendler[b,*]

Ruthenium modified cobalt oxides were prepared by 1) impregnating ruthenium chloride hydrate on cobalt oxides, Ru-supported catalysts (Ru/Co_3O_4) and 2) Ru-doped catalysts ($Ru-Co_3O_4$), where the ruthenium ions were added to the pre-cursor solution, by one-step sol-gel method with cobalt nitrate. The physicochemical properties of the catalysts were characterized by ICP, BET, XRD, HR-TEM, TPR and XPS analysis. The effects of ruthenium have been studied for the total oxidation of vinyl chloride. This Ru modifier is observed to enhance oxygenate formation. The difficult prepared methods make contribution to the different amount of Ru^{4+} on the surface of the catalysts. While, Ru^{4+} will be in synergy with Co^{2+} concentration, and this would also change the chemical coordination of oxygen on the surface. The dispersion of Ru oxides on the cobalt oxides surface not only could improve the catalytic activity and stability on steam, but also decrease the amount of chlorinated by-products and increase the HCl selectivity.

Introduction

Recently, several legislations concerning various pollutants have as a major objective the improvement of air quality. Volatile organic compounds (VOCs), which emitted from heavy widespread applications in industry, are significant atmospheric pollutants owing to their high toxicity and malodorous nature. Among VOCs, especially chlorinated VOCs (such as dichloromethane, chloroform, carbon tetrachloride, 1,2-dichloromethane, trichloroethylene, tetrachloroethylene) require special attention on account of extreme stability.[1] One of the principal solutions to reduce the emission is the catalytic oxidation technique,[2] which offers the possibility of removing them from aerial effluents at low temperature in more economical process than other technologies. In addition, with this technique, chlorinated VOCs could be completely oxidized into CO_2, H_2O, Cl_2 or HCl, which are low toxicity final products.[3] In general, noble metals such as platinum, palladium, gold, and rhodium are dispersed on supports with high specific surface areas,[4-7] which are well established as efficient catalysts for VOCs oxidation.[8] They are very reactive in the complete oxidation and can avoid the formation of by-products.[9] However, it becomes necessary to optimize the composition of

the catalysts in order to obtain lower supported content catalysts because of the high cost.[10]

Many researches have certified that single or mixed transition metal oxides could have an excellent catalytic activity and stability for total oxidation of VOCs.[11] Also, the noble metal based catalysts perform high specific activity, resistance to deactivation and ability to be regenerated, without considering its expensive costs. Among these oxides, cobalt oxides catalysts have been reported to be effective on low-temperature oxidation of carbon monoxide,[12] hydrocarbons,[13] and diesel soot.[14] Active behavior of Co_3O_4 catalysts is most likely related to high bulk oxygen mobility and the easy formation of highly active oxygen species. On the other hand, ruthenium catalysts have received much attention over the past years, because of its high activity in oxidation and reduction reactions, especially in oxidation of hydrogen chloride to chlorine in industry.[15] Supported ruthenium catalysts offer good reactivity in various catalytic reactions such as methane,[16] ammonia oxidation[17], CO oxidation,[18] steam reforming,[19, 20] and reduction of NO by methane.[21] Another important reason, under oxidation conditions, Ru transformed to Ru dioxide also shows highly desirable reactivity and stability, which decrease the cost comparing to the other noble metals. Previous reports have investigated these catalysts, such as $Ru-CeO_2$,[22] Ru/Al_2O_3,[23] and Ru/TiO_2,[24] showing a very good activity and chemical stability in chlorinated hydrocarbons oxidation.

Large amounts of vinyl chloride (VC), as a model chlorinated VOCs, are released in the chloralkali industrial process, which is greatly harmful to environment and public health. In the

[a.] Key Laboratory for Advanced Materials, Research Institute of Industrial Catalysis, East China University of Science and Technology, Shanghai 200237, P.R. China E-mail: ylguo@ecust.edu.cn (Y.L. GUO)

[b.] Institut de recherches sur la catalyse et l'environnement de Lyon, UMR 5256-CNRS, Université Lyon 1, 2 avenue Albert Einstein, 69626 Villeurbanne Cedex, France E-mail: anne.giroir-fendler@ircelyon.univ-lyon1.fr (A. GIROIR-FENDLER)

RSC Advances Accepted Manuscript

recent studies, the chlorine species adsorbed on the active surface sites could be removed via the Deacon reaction on RuO_2.[25] Therefore, the association of ruthenium and cobalt oxides, which combine the highly active oxygen species with the ability for chlorine activation, can establish a successful catalytic system in VC oxidation reactions. The catalytic performances of supported noble metals are strongly depended on the preparation method, the metal loading and, as a consequence, the physicochemical properties.[8]

In this work, Ru modified Co_3O_4, including doped and supported, were synthesized, characterized and tested on the VC oxidation. The concentration of chlorinated by-products was studied during the oxidation process. The effects by different preparation method had an influence between the ruthenium and cobalt species, which involved the Co^{2+} and Ru^{4+} dispersion. The relationship between ruthenium with cobalt structural features and the catalytic activity was investigated. Better performance on activity and stability will provide the challenge on the industrial application in the future for environmental protection.

Experimental

Catalysts preparation

Pure Co_3O_4 oxide was prepared via a conventional citrate sol-gel method. Typically, stoichiometric amounts of citric acid (CA) was added to an aqueous cobalt salt solution using $Co(NO_3)_2 \cdot 6H_2O$ as the precursor with a molar ratio of CA/Co equal to 1.1. The mixture was heated to 80 ^oC under magnetic stirring to completely dissolve the CA and maintained at this temperature to evaporate excess amount of H_2O until the formation of a viscous gel. After dried at 100 ^oC for 10 h in an oven, the resulting material was finally calcined at 450 ^oC (the heating rate of 1 ^oC min^{-1}) for 4 h under the air atmosphere and then cooled down.

Ru-supported Co_3O_4 catalysts (noted as Ru/Co_3O_4) were prepared by an optimized impregnation method. Certain amounts of $RuCl_3$ as the precursor was dissolved in an ethanol aqueous solution with the ratio of ethanol to water 1:4, then the previously prepared Co_3O_4 oxide was added into this solution, following evaporated at 80 ^oC under magnetic stirring and then dried at 100 ^oC for 10 h in an oven. After that, the catalysts were calcined under the same condition as above.

Ru-doped Co_3O_4 catalysts (noted as $Ru-Co_3O_4$) were prepared by the same sol-gel method as that of pure Co_3O_4 oxide, where an aqueous solution containing a certain amount of $Co(NO_3)_2 \cdot 6H_2O$ and $RuCl_3$ as precursors.

For a comparison, Ru supported on a commercial SiO_2 oxide was prepared by the same impregnation method as that of Ru/Co_3O_4 as reference. Additionally, for a facile description, the Ru modified catalysts were denoted as X% Ru/Co_3O_4, X% $Ru-Co_3O_4$ and X% Ru/SiO_2, respectively, where X represented the weight percentage of Ru in the catalyst.

Catalysts characterization

The contents of Ru in the prepared catalysts were quantitatively determined by inductively coupled plasma atomic emission spectroscopy (ICP-AES) on a Varian 710ES instrument. Before the measurement, the metal oxides were dissolved using a mixture of inorganic acids (H_2SO_4, HNO_3 and HF).

Powder X-ray diffraction (XRD) patterns of these catalysts were recorded on a Bruker AXS D8 Focus diffractometer with Cu Kα (λ=0.154056nm) radiation at 40 kV and 40 mA. The scan range was from 10 to 80° (2θ) with a step size of 0.02^o and a scanning rate of 0.6^o min^{-1}. The lattice parameter and crystallite size of each catalyst were calculated according to the XRD rietveld refinement using the Topas4 software.

The nitrogen adsorption-desorption isotherms were measured at 77 K on a Micromeritics ASAP 2020M surface area & porosity analyzer. The specific surface area (SSA) of each catalyst was obtained by the Brunauer-Emmett-Teller (BET) method.

The redox properties of these catalysts were analyzed by temperature-programmed reduction of H_2 (H_2-TPR) on a Micromeritics AutoChemII 2920 sorption instrument. In a typical run, 0.10 g of the catalyst placed in a quartz reactor was pretreated at 450 ^oC for 30 min with a gas flow of 3vol.% O_2/He. After cooled down to room temperature, the reducing gas (10vol.% H_2/Ar) with a flow rate of 50 ml·min^{-1} was introduced into the reactor under the heating from 25 to 800 °C at a rate of 10 °C·min^{-1}. The signal of H_2 uptake in the H_2-TPR was collected by a thermal conductivity detector (TCD) after a cold trap to remove the produced water.

X-ray photoelectron spectroscopy (XPS) analysis was carried out on a Thermo Fisher ESCALAB 250Xi electron spectrometer with an AlKα (1486.6 eV) radiation source. The constant charging of the XPS spectra was corrected by C1s of adventitious carbon with binding energy of 284.8 eV.

Transmission electron microscopy (TEM) observations of the catalysts were performed on a FEI Tecnai G2 F30 microscope with STEM-EDX detector. The specimens for TEM were prepared by grinding of the powdered catalyst in a mortar, dispersing it in ethanol and placing a droplet of the suspension onto a copper grid coated with a carbon film.

Catalytic testing

The catalytic reaction of VC oxidation was carried out in a quartz tubular fixed-bed flow reactor (inner diameter = 6 mm) under atmospheric pressure. In each experiment, 0.60 g of the catalyst (pellets with diameter from 0.3 to 0.45 mm), was placed in the reactor. The feed gas (120 ml·min^{-1}) with VC concentration of 1000 ppm diluted by air, was passed through the catalyst bed, corresponding to a gas hourly space velocity (GHSV) at 15000 h^{-1}. A K-type thermocouple was placed in the catalyst bed to monitor the reaction temperature heated in the range of 50-350 ^oC.

The gas effluent was analyzed by an online PerkinElmer Clarus 580 gas chromatograph (GC) equipped with a flame ionization detector (FID) during stepwise increase in the reaction temperature, usually after 30 min at the selected temperature to achieve the steady state. In addition, a PerkinElmer TurboMatrix 650 thermal desorber combined with an Agilent 5975C

inert mass spectrum was used for the trapping and qualitative determination of the possible Cl-containing by-products, such as CH_2Cl-$CHCl_2$, CH_2Cl_2, $CHCl_3$, CCl_4.

The VC conversion and HCl selectivity was calculated according to the following equations:

$$\text{VC Conversion (\%)} = \frac{[VC]_{in} - [VC]_{out}}{[VC]_{in}} \cdot 100$$

$$\text{HCl Selectivity (\%)} = 100 - \frac{4[CCl_4]}{10} - \frac{3([CHCl_2CH_2Cl] + [CHCl_3])}{10} - \frac{2[CH_2Cl_2]}{10}$$

where $[VC]_{in}$, $[VC]_{out}$, $[CCl_4]$, $[CHCl_2CH_2Cl]$, $[CHCl_3]$ and $[CH_2Cl_2]$ represented the VC concentrations in the inlet and outlet as well as the concentration of CCl_4, $CHCl_2CH_2Cl$, $CHCl_3$ and CH_2Cl_2 in the effluent gas, respectively.

Results and discussion

The actual Ru content and the physicochemical properties of Ru modified catalysts are listed in Table 1. All the catalysts presented a close weight percent to the nominal one. The XRD patterns of all prepared catalysts are showed in Fig. 1, and crystalline phase identification is performed by referring to the standard powder diffraction file (PDF). Notably, all catalysts presented characteristic reflection peaks of cubic spinel Co_3O_4 oxides (*Fd-3m*, JCPDS #42-1467) at 2θ of 19.0^o, 31.2^o, 36.8^o, 44.8^o, 59.4^o, and 65.2^o corresponding to the (111), (220), (311), (400), (511), and (440) crystal faces, respectively.[26, 27] No

diffraction peaks attributable to the CoO phase detected.[28] In addition, there was no observation of the feature patterns related to Ru oxides in the region of 25-42° in all Ru modified catalysts, which could be due to the low amounts of Ru species on these catalysts and/or the lower intensity of Ru peaks than the Co oxides ones. The lattice parameters of Co_3O_4 structure and the crystallite sizes of all catalysts are calculated by Topas 4.0 program and listed in Table 1. The lattice parameters of Ru-doped catalysts (0.5%Ru-Co_3O_4 and 1%Ru-Co_3O_4) increased compared with pure Co_3O_4 from 8.0844 to 8.0896 Å. This could be attributed to the substitution effect of Ru ions into cubic lattice Co_3O_4 spinel, which results in a lattice parameter increased with after the metal incorporation in doped ones.[29] However, Ru-supported catalysts (0.5%Ru/Co_3O_4 and 1%Ru/Co_3O_4) give no obvious change in parameter, about 8.8046 or 8.0847 Å, which could be due to the Ru particles dispersed on the surface of cobalt oxides without changing the lattice parameter. The crystalline size was increased from 27.8 nm on pure Co_3O_4 to ~32 nm and ~39 nm on Ru-Co_3O_4 and Ru/Co_3O_4, respectively. While, the BET surface areas of all catalysts were in the range of 20-29 $m^2 \cdot g^{-1}$ without any obvious difference in Table 1.

TEM images and EDX-mapping images of 1%Ru-Co_3O_4 and 1%Ru/Co_3O_4 catalysts are shown in Fig. 2 and Fig. 3. It can be observed that both catalysts were nano-scaled particles, showing the characteristic lattice fringes of the cobalt oxide. The dark regions were presented on the 1%Ru/Co_3O_4 (Fig. 2 b) could be associated to the formation of RuO_2 crystalline phase on the surface, leading to a lower resolution of these lattice fringes of Co_3O_4 compared with that on 1%Ru-Co_3O_4 (Fig. 2 a). Based on the analysis of the EDX-mapping images (Fig. 3 a and

Fig. 1 XRD patterns of all catalysts.
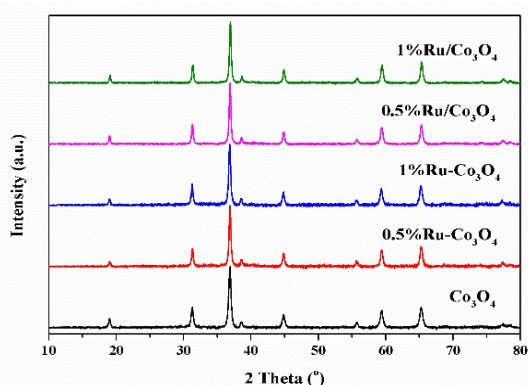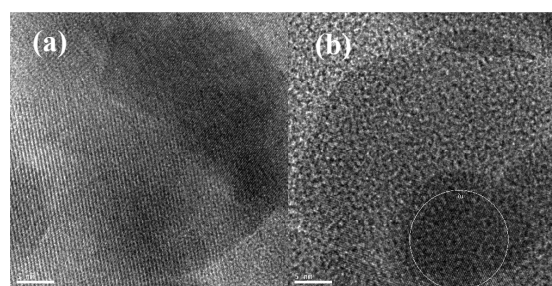

Fig. 2 TEM images of 1%Ru-Co_3O_4 (a) and 1%Ru/Co_3O4 (b).

Table 1. Physico-chemical properties of the catalysts.

Catalysts	Ru loading [a] (wt. %)	Lattice parameter [b] (Å)	Crystalline size [c] (nm)	S_{BET} [d] (m^2g^{-1})
Co_3O_4	-	8.0844	27.8	20
0.5%Ru-Co_3O_4	0.48	8.0873	32.4	26
1%Ru-Co_3O_4	0.98	8.0896	31.6	29
0.5%Ru/Co_3O_4	0.49	8.0847	39.3	24
1%Ru/Co_3O_4	0.97	8.0846	39.9	23

[a] Measured by ICP-AES.

[b,c] Lattice parameters and crystallite sizes calculated in Topas 4.0 program.

[d] Surface area determined from N_2 isotherm.

ARTICLE

Journal Name

Fig.3 b), it can be observed the high distribution density of Ru element on the surface of 1%Ru/Co_3O_4. Contrarily, only trace of surface Ru species was detected on 1%Ru-Co_3O_4 with the same total quantity of Ru in bulk domains. These findings indicated that the Ru species were well dispersed on the surface of cobalt oxides in 1%Ru/Co_3O_4, while mostly of Ru was preferentially doped into the crystalline lattice of cobalt oxides on 1%Ru-Co_3O_4, according to the XRD results.

The redox properties of all catalysts are analyzed by H_2-TPR. As shown in Fig. 4, the H_2-TPR profiles can be generally divided into two regions according to the varied reduction temperature, which was assigned to the change of different reduction species on the catalysts. For the pure Co_3O_4 catalyst, the first reduction peak centered at 256 ^{o}C was associated with the reduction of Co^{3+} into Co^{2+}, while the second peak centered at 351°C was attributed to further reduction of Co^{2+} into metallic cobalt.[30] It is accepted that the reduction of ruthenium ions (Ru^{4+} or Ru^{2+}) into metallic species (Ru^0) usually takes place at a lower temperature in comparison with the occurrence of Co_3O_4 reduction.[31] According to the literature, ruthenium (IV) in RuO_2 could be reduced in several steps from 97 ^{o}C to 176 ^{o}C.[32] However, it was difficult to observe the

separate reduced peaks assignable to ruthenium ions over the catalysts because of its relatively lower content of surface ruthenium ions. Moreover, the reducible behaviors of ruthenium induced by their location in Co_3O_4 lattice probably being overlapped with the reduction peaks of Co_3O_4 at the low temperature.[33] Notably, the reduction temperatures of peaks maximum over all Ru modified catalysts was shifted to lower temperature range compared to the pure Co_3O_4, indicating that the addition of ruthenium markedly facilitated the reduction of cobalt species. Especially, Ru-supported catalysts exhibited even better reducible behaviors than the Ru-doped catalysts, from 227 ^{o}C to 182 ^{o}C in 0.5% Ru catalysts, and from 186 ^{o}C to 145 ^{o}C in 1 %Ru catalysts, respectively. The first reduced peaks shifted to lower temperature, which could be associated to that Ru improve the reduction of Co^{3+} into Co^{2+}. The more quantity of ruthenium ions distributed on the surface of cobalt oxide, the more ability to improve reduction[34]. On the other hand, it is propose that the surface RuO_x nanoparticles are preferentially reduced at low temperature than cobalt oxides.[35] Atomic hydrogen, which is generated by dissociation on the Ru^0 reduction nuclei, will smoothly spread to the neighboring Co_3O_4 particles to accelerate their reduction.[36] This phenomenon, called hydrogen spillover effect, will noticeably decrease the reduction temperatures. From the results above, it could be known that Ru has a strong interaction with the Co_3O_4 layer. Overall, the relative low-temperature reducibility of all catalysts from the highest to the lowest, which was derived from H_2-TPR analysis, followed the order of 1%Ru/Co_3O_4 > 0.5%Ru/Co_3O_4 > 1%Ru-Co_3O_4 > 0.5%Ru-Co_3O_4 > Co_3O_4.

All catalysts were analyzed by XPS technique in order to investigate the surface element compositions, the metal oxidation states and the nature of the oxygen species. Considering that the binding energy (BE) of Ru3d is very close to that of C1s,[37] the Ru oxidation states are determined by the Ru3p spectra. As illustrated in Fig. 5, the Ru-doped catalysts showed lower spectra intensities than the Ru-supported catalysts, verifying that low contents of residual Ru species were present on catalysts surface, which could be attributed
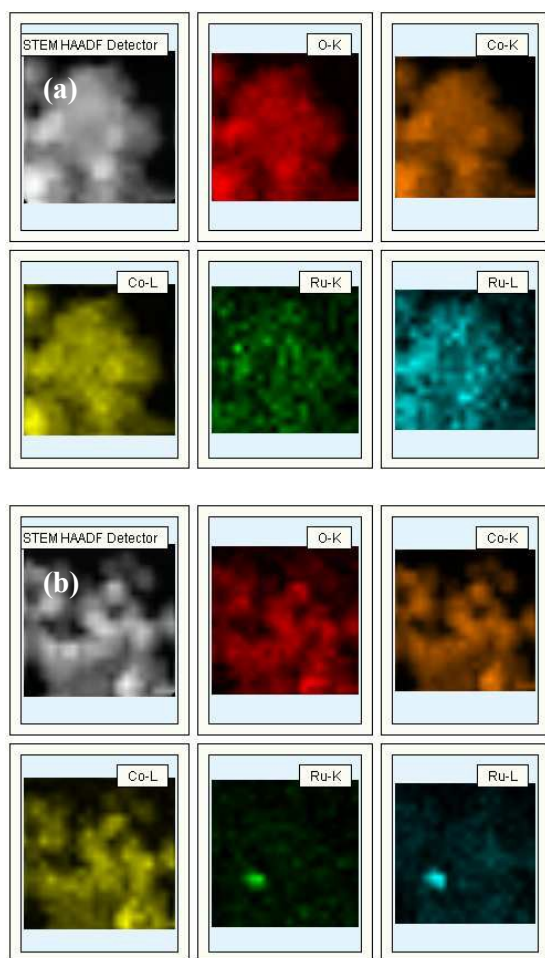

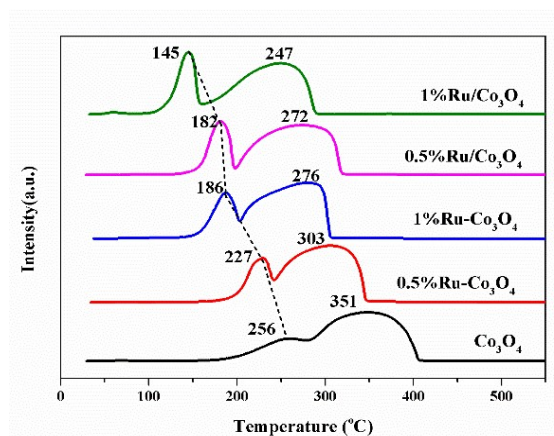**Fig. 3** EDX-mapping of 1%Ru-Co_3O_4 (a) and 1%Ru/Co_3O_4 (b).

Fig. 4 H_2-TPR profiles of all catalysts.

RSC Advances

to the Ru introduction into Co_3O_4 framework. Additionally, the XPS spectra can be deconvoluted into three peaks located at 461.6, 463.4 and 466.3 eV, which could be assigned to the metallic Ru, Ru^{4+} and Ru^{6+} species, respectively.[37, 38] The atomic molar ratios of surface Ru^{4+} species (Ru^{4+}/Ru) are determined and listed in Table 2.
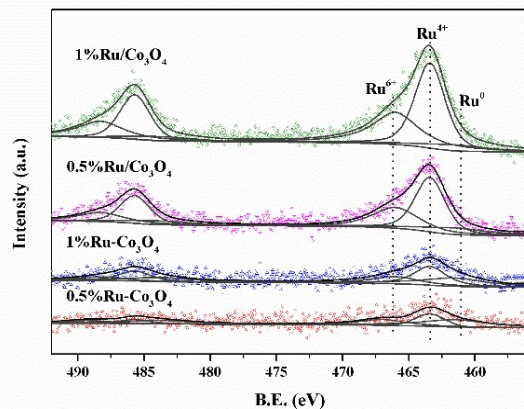

Fig. 5 Ru 3p XPS spectra of all catalysts.
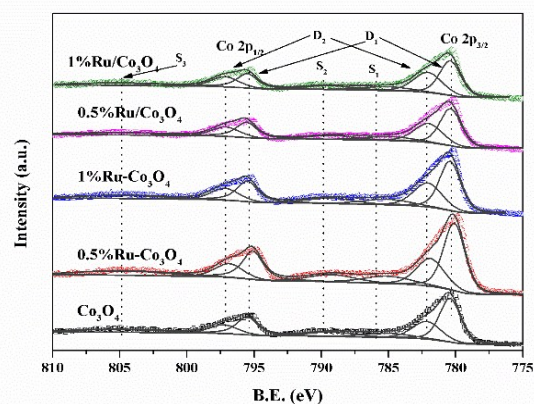

Fig. 6 Co2p XPS spectra of all catalysts.

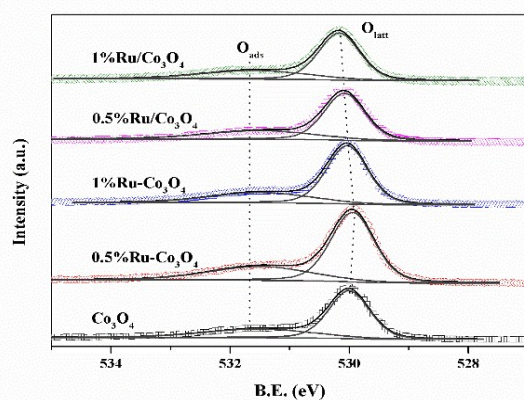

Fig. 7 O1s XPS spectra of all catalysts.

Table 2. Atomic surface ratios and surface composition of the catalysts.

Catalysts	Ru^{4+}/Ru (at.%)	$Co^{3+}/Co^{2+\,a}$ (at./at.)	O_{ads}/O_{latt} (at.%)
Co_3O_4	-	1.85	49.8
0.5%Ru-Co_3O_4	25.5	1.84	47.0
1%Ru-Co_3O_4	38.9	1.54	44.1
0.5%Ru/Co_3O_4	50.5	1.47	49.8
1%Ru/Co_3O_4	52.1	1.26	48.8

^{a} Co^{3+}/Co^{2+} = $D_1(Co2p_{3/2})$ /$D_2(Co2p_{3/2})$.

It was observed that the order in terms of Ru^{4+} atomic molar ratio from the highest to the lowest was 1%Ru/Co_3O_4 (52.1%) > 0.5%Ru/Co_3O_4 (50.5%) > 1%Ru-Co_3O_4 (38.9） > 0.5%Ru-Co_3O_4 (25.5%), where the Ru-supported catalysts possessed more abundant surface Ru^{4+} species than the Ru-doped catalysts. In addition, the Co2p XPS spectra of all catalysts is shown in Fig. 6. For the Co_3O_4 oxide, the BE value of $Co2p_{3/2}$ is around 779.8 eV with a spin-orbital splitting of 15.1 eV. Herein, the Co2p spectra of all catalysts were deconvoluted into two spin-orbit doublets Co^{3+} (D_1) and Co^{2+} (D_2) as well as three satellite peaks (S_1, S_2, S_3).[30, 39-41] Moreover, the pure Co_3O_4 presented the normal molar ratio of Co^{3+}/Co^{2+} (1.85, in Table 2)[42], while the Co^{3+}/Co^{2+} ratio decreased down to the range of 1.84-1.26 over the Ru doped and supported catalysts, indicating the reduction of Co^{3+} into Co^{2+} due to the interaction of Ru species with Co_3O_4 spinel structure.[43]

The O1s spectra of all catalystsise presented in Fig. 7, which is mainly deconvoluted into two peaks corresponding to different oxygen species on the catalysts. As previously reported, the peaks at BE of 529.9-530.2 and 531.4-531.6 eV were characteristic of lattice oxygen (O_{latt}, i.e. O^{2-}) and surface adsorbed oxygen (O_{ads}, i.e. OH group, O^- or O_2^{2-}), respectively.[44, 45] The surface oxygen specie O_{ads}/O_{latt} ratio was decreased from 49.8% to 44.1% in Ru-doped catalysts, whereas the Ru-supported catalysts presented nearly the
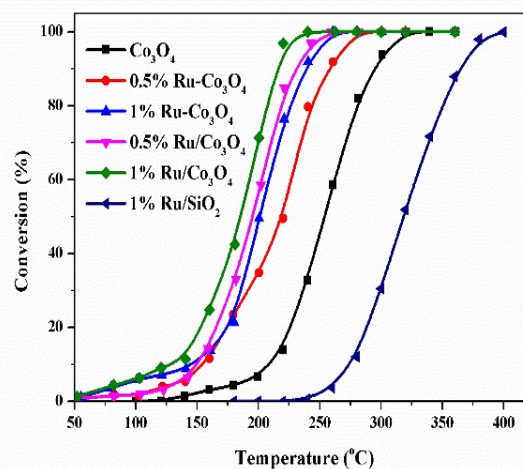

Fig. 8 The light-off curves as a function of reaction temperature for VC oxidation.

Table 3. Light-off temperatures at 50% and 90% of VC conversion.

| Catalysts	T50 [a] (^{o}C)	T90 (^{o}C)
Co_3O_4	253	295
0.5%Ru-Co_3O_4	218	258
1%Ru-Co_3O_4	199	238
0.5%Ru/Co_3O_4	193	231
1%Ru/Co_3O_4	186	216

[a] The temperature of conversion at 50% and 90%.

same ratio with Co_3O_4 (from 49.8% to 48.8%). Besides, binding energy of O_{latt} slightly increases, which is also a correlation to Co^{2+} concentration on the surface.[42]

The catalytic performances of Co_3O_4 and Ru modified Co_3O_4 catalysts for VC oxidation were evaluated. The light-off curves of VC conversion as a function of reaction temperature are shown in Fig. 8, and the T_{50} and T_{90} values corresponding to the temperatures at 50 and 90% of VC conversion are listed in Table 3.

It could be found that 1%RuO_2/SiO_2 as reference possessed the poorest catalytic activity of VC oxidation with a complete conversion of VC achieved at 400 ^{o}C. However, all of those Ru modified Co_3O_4 catalysts exhibited higher catalytic activities for VC oxidation than the pure Co_3O_4 and reference catalyst. The catalyst of 1%Ru/Co_3O_4 was proved to be the optimum one with the lowest T_{50} and T_{90}. These results indicated that single Ru oxide was inactive at low temperature for the oxidative destruction of VC, and Co_3O_4 was the predominant active component for the reaction over Ru modified Co_3O_4 catalysts. Furthermore, the catalytic activities according to the T_{50} and T_{90} values from the highest to lowest followed the order of 1%Ru/Co_3O_4 > 0.5%Ru/Co_3O_4 > 1%Ru-Co_3O_4 > 0.5%Ru-Co_3O_4 > Co_3O_4 > 1%Ru/SiO_2, which was consistent with the sequence of redox ability obtained in H_2-TPR.

According to the results, it could be deduced that the Ru species not only affected the redox property of Co_3O_4, but also played a particular role in the reaction. The catalytic activity should be associated to lower temperature reducibility, which
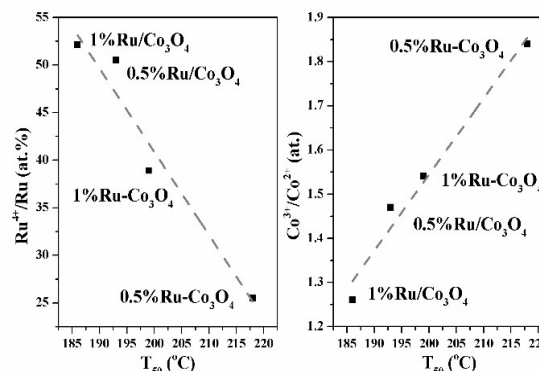
Fig. 9 The linear relationship between T_{50} and Ru^{4+}/Ru, Co^{3+}/Co^{2+}.

is caused by Ru dispersed on the cobalt surface and an increased Ru^{4+}/Ru content. Moreover the Co^{3+} was replaced by Co^{2+} or Ru^{4+} causing higher concentration of surface Co^{2+}, which indicative of oxygen defects, increasing the higher intrinsic activity.[46] A linear relationship between T_{50} and Ru^{4+}/Ru with Co^{3+}/Co^{2+} is showed in Fig.9. Thus, the catalytic activity has a positive correlation to the surface Ru^{4+} amount, and a negative correlation with the surface Co^{3+}/Co^{2+} ratio. Compared with other supported noble metal catalysts, listed in Table 4,[22, 24, 25] ruthenium supported cobalt oxides catalyst showed a good catalytic performance on chlorinated VOCs oxidation.

As it is well known a highly chlorinated by-products can be yielded in the reaction of CVOCs oxidation.[47] Therefore, it is reasonable to provide the experimental information about the selectivity to the ideal completely oxidation products (namely H_2O, CO_2 and HCl or Cl_2) and, more particularly, the concentrations of by-products. In this work, the possible chlorinated organics in the effluent feed were quantitatively determined in the catalytic test. During the stepwise increase temperature oxidation process, 1,1,2-trichloroethane (CH_2Cl-$CHCl_2$), dichloromethane (CH_2Cl_2), trichloromethane ($CHCl_3$)

Table 4. Catalytic performances for VOCs on supported noble metals catalysts reported in the literature.

Catalysts	Conditions[a]	Chlorinated VOCs conversion[b]	Reference
1%Ru-CeO_2		T_{50}=204, T_{90}=250	
1%Ru/CeO_2	CB=550 ppm	T_{50}=217, T_{90}=250	[22]
1%Ru/SBA-15	GHSV=15,000 h^{-1}	T_{50}=312, T_{90}=350	
1%Ru/TiO_2	DCM=750 ppm[c]	T_{50}=235, T_{90}=267	[24]
1%Ru/Al_2O_3	GHSV=10,000 h^{-1}	T_{50}=276, T_{90}=308	
0.4%Ru/CeO2-r[d]		T_{50}=230, T_{90}=275	
0.4%Ru/CeO2-c	CB=1000ppm	T_{50}=,250 T_{90}=306	[25]
0.4%Ru/CeO2-o	GHSV=30,000 h^{-1}	T_{50}=320, T_{90}=363	
0.5%Ru/Co_3O_4	VC=1000ppm	T_{50}=193, T_{90}=231	This work
1%Ru/Co_3O_4	GHSV=15,000 h^{-1}	T_{50}=186, T_{90}=216	

[a] Chlorobenzene (CB), dichloromethane (DCE), vinyl chloride (VC).

[b] The temperature of conversion at 50% and 90%.

[c] 10%O_2 and N_2 balance.

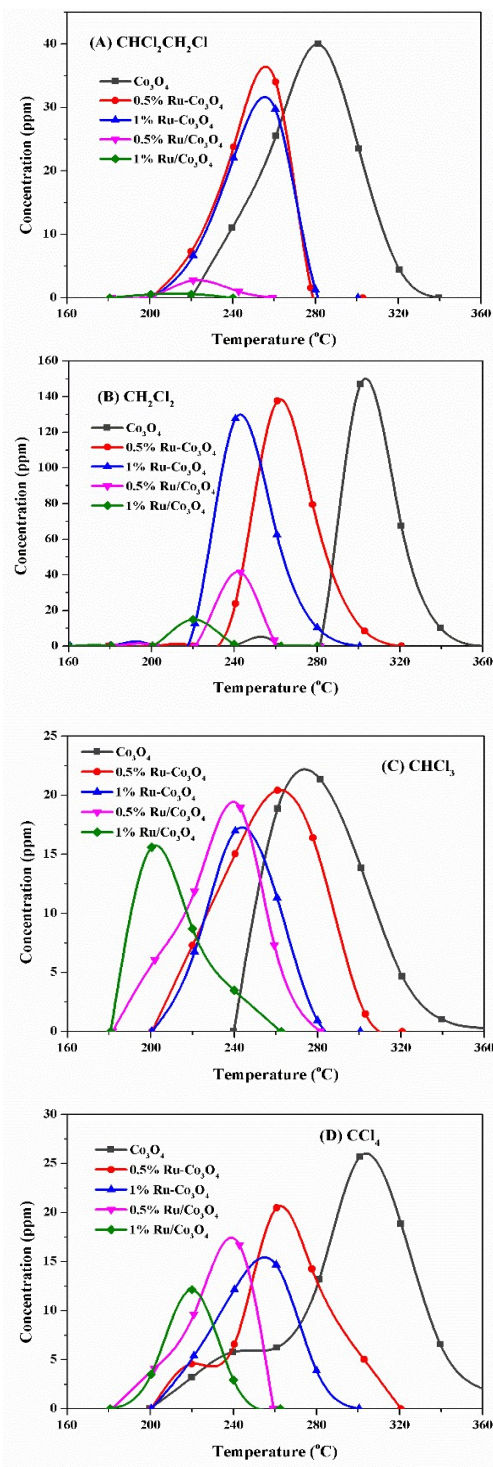[d] CeO_2 nanorods (-r), CeO_2 nanocubes (-c), CeO_2 nano-octahedra (-o).

Fig. 10 The concentrations of chlorinated organics as a function of reaction temperature, (A) CHCl$_2$CH$_2$Cl (B) CH$_2$Cl$_2$ (C) CHCl$_3$ (D) CCl$_4$.

and tetrachloromethane (CCl$_4$) are the major chlorinated by-products,[48] and their concentrations as a function of reaction temperature over all prepared catalysts are shown in Fig. 10. The significant amounts of chlorinated by-products were

formed at the temperature range of 160-360°C. The concentrations of these chlorinated organics over 1%Ru/Co$_3$O$_4$ were lower than those over any other catalysts, which could be attributed to its optimum low-temperature catalytic activity in the reaction.

Additionally, an unexpected high amount of CH$_2$Cl$_2$ was detected, in Fig. 10 (B), when the VC conversion was achieved at about 95% (Fig. 8) over all catalysts. And it quickly decreased with the reaction temperature increased. During the reaction, CH$_2$Cl-CHCl$_2$ may be produced by chlorinate-addition reaction to vinyl chloride, and then be cracked into CH$_2$Cl$_2$ and CHCl$_3$ by thermally decomposed. At last, CCl$_4$ could be formed as a result of the further chlorination of CH$_2$Cl$_2$ or CHCl$_3$. This phenomenon is observed between the Ru doped and supported cobalt oxide is the distribution concentration of chlorinated by-products. Ru-supported catalysts present a lower concentration of CH$_2$Cl-CHCl$_2$, which will form low concentration of CH$_2$Cl$_2$ and CHCl$_3$. However, the Ru-doped catalysts only change the reaction activity and have a little effect on chlorinated by-products, which show the same tendency with pure Co$_3$O$_4$. However, it seems that RuO$_2$ dispersed on the surface have a better performance on restraining the chloride addition reaction of vinyl chloride.

The hydrogen chloride (HCl) selectivity was evaluated in order to understand the final product in the VC oxidation, in Fig. 11. It should be pointed out that all chlorinated compounds were dechlorinated into HCl without any chlorinated byproducts detected at higher temperature over all catalysts.[49] Because Cl$_2$ was not detected during the oxidation, the HCl selectivity gradually decreased with the rise of reaction temperature due to the formation of chlorinated by-products. Then, when VC conversion reached around 95%, lowest HCl selectivity was obtained, simultaneously accompanied by the formation of high amounts of chlorinated by-products. With reaction temperature continuously increase, HCl selectivity raised back to near 100%, corresponding to the diminished concentrations of these chlorinated organics. It can be observed that 1%Ru/Co$_3$O$_4$ exhibited the minimum change in HCl selectivity among all catalysts, which was also attributed to its best catalytic activity for VC oxidation.

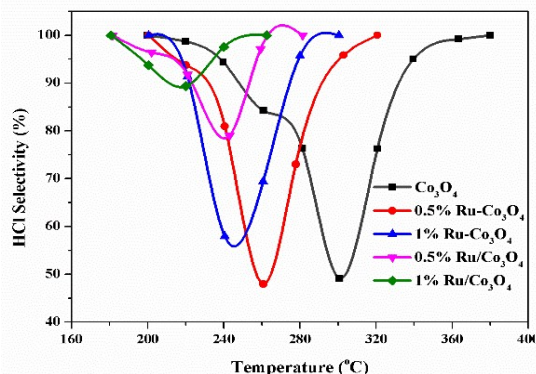Moreover, the catalytic stability in long-term test without

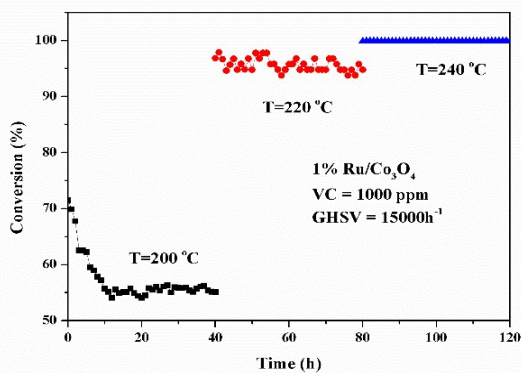Fig. 11 Selectivity (%) to HCl over all the catalysts.

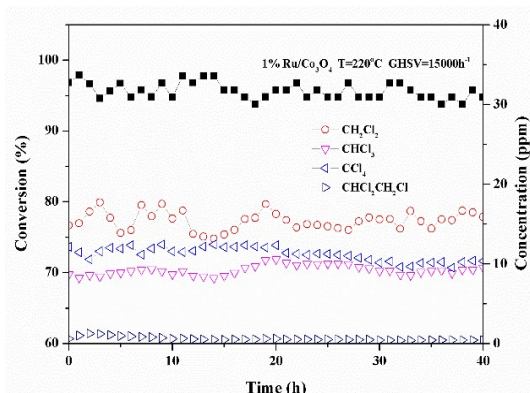Fig. 12 Lifetime test conducted on different temperature.

Fig. 13 Lifetime test performed with 1%Ru/Co$_3$O$_4$ at 220 ^{o}C.

deactivation is also important, which was evaluated over 1%Ru/Co$_3$O$_4$, as the optimum catalyst, at various reaction temperatures for 120 hours (40 hours for each specific temperature 200 ^{o}C, 220 ^{o}C, and 240 ^{o}C with the same catalyst). The corresponding profiles of VC conversion as a function of time on stream are illustrated in Fig. 12. It can be observed that 1%Ru/Co$_3$O$_4$ exhibited relatively poor catalytic stability at low temperature (200 ^{o}C). Indeed, VC conversion decreased from 72% to 63% during the first 5 hours, indicating the occurrence of gradual deactivation on the catalyst,[50] and finally VC conversion reached a steady value of about 55% till the end of time. However, it was very stable when the temperature reached to 220 ^{o}C or 240 ^{o}C and an even higher temperature.

Meanwhile, the concentration of those chlorinated by-products in the stability test at 220 ^{o}C was also determined and shown in Fig. 13. In spite of the presence of some fluctuations, VC conversion was achieved stable about 95% at 220 ^{o}C during the first 40 hours test, and the formation of CHCl$_3$, CCl$_4$, CH$_2$Cl$_2$ as the main chlorinated organics was unavoidable with the concentrations about 10, 15, 8 ppm, respectively. However, at higher reaction temperature of 260 ^{o}C (shown in Fig. 10), 1%Ru/Co$_3$O$_4$ showed excellent catalytic

activity and stability with a complete VC conversion and an absence of chlorinated by-products formation.

Conclusions

All Ru modified Co$_3$O$_4$ presented an improved catalytic activity and HCl selectivity, decreasing the undesirable chloride by-products formation, compared to Co$_3$O$_4$ and 1%Ru/SiO$_2$. Moreover, it clearly demonstrates the difference between the Ru supported and doped catalysts, where the supported ones presented the highest catalytic performance. These supported catalysts presented a better performance on the reaction activity. Thus, this high catalytic activity could be attributed to high reducibility of Co oxides, and also to the complex interplay between Ru species on the surface and Co$_3$O$_4$ phase composition. Thus, the substitution of Ru species for Co^{3+} in spinel structure with low amount on the surface of the supported catalysts can increase Co^{2+} concentration. High relative proportion of Co^{2+} and Ru^{4+}, which will also devote to oxygen defects or vacancies, will not only increase the catalytic activity but also decrease the amounts of chlorinated by-products and increased the HCl selectivity.

Acknowledgements

Notes and references

‡ Footnotes relating to the main text should appear here. These might include comments relevant to but not central to the matter under discussion, limited experimental and spectral data, and crystallographic data.

1.   P. Wolkoff and G. D. Nielsen, *Atmos. Environ.*, 2001, **35**, 4407-4417.
2.   J. J. Spivey, *Ind. Eng. Chem. Res.*, 1987, **26**, 2165-2180.
3.   B. de Rivas, R. López-Fonseca, M. A. Gutiérrez-Ortiz and J. I. Gutiérrez-Ortiz, *Appl. Catal., B*, 2011, **104**, 373-381.
4.   K. Okumura, T. Kobayashi, H. Tanaka and M. Niwa, *Appl. Catal., B*, 2003, **44**, 325-331.
5.   S. Scirè, S. Minicò, C. Crisafulli, C. Satriano and A. Pistone, *Appl. Catal., B*, 2003, **40**, 43-49.
6.   F. J. Maldonado-Hódar, C. Moreno-Castilla and A. F. Pérez-Cadenas, *Appl. Catal., B*, 2004, **54**, 217-224.
7.   O. Demoulin, B. Le Clef, M. Navez and P. Ruiz, *Appl. Catal., A*, 2008, **344**, 1-9.
8.   L. F. Liotta, *Appl. Catal., B*, 2010, **100**, 403-412.

View Article Online
DOI: 10.1039/C6RA18503G

ARTICLE

9. D. Homsi, S. Aouad, J. El Nakat, B. El Khoury, P. Obeid, E. Abi-Aad and A. Aboukaïs, *Catal. Commun.*, 2011, **12**, 776-780.

10. S. Aouad, E. Abi-Aad and A. Aboukaïs, *Appl. Catal., B*, 2009, **88**, 249-256.

11. W. B. Li, J. X. Wang and H. Gong, *Catal. Today*, 2009, **148**, 81-87.

12. X. Xie, Y. Li, Z.-Q. Liu, M. Haruta and W. Shen, *Nature*, 2009, **458**, 746-749.

13. Q. Liu, L.-C. Wang, M. Chen, Y. Cao, H.-Y. He and K.-N. Fan, *J. Catal.*, 2009, **263**, 104-113.

14. M. Sun, L. Wang, B. Feng, Z. Zhang, G. Lu and Y. Guo, *Catal. Today*, 2011, **175**, 100-105.

15. N. López, J. Gómez-Segura, R. P. Marín and J. Pérez-Ramírez, *J. Catal.*, 2008, **255**, 29-39.

16. Y. Liu, F.-Y. Huang, J.-M. Li, W.-Z. Weng, C.-R. Luo, M.-L. Wang, W.-S. Xia, C.-J. Huang and H.-L. Wan, *J. Catal.*, 2008, **256**, 192-203.

17. Y. Wang, K. Jacobi, W. D. Schöne and G. Ertl, *J. Phys. Chem. B*, 2005, **109**, 7883-7893.

18. J. Assmann, V. Narkhede, N. A. Breuer, M. Muhler, A. P. Seitsonen, M. Knapp, D. Crihan, A. Farkas, G. Mellau and H. Over, *J. Phys.: Condens. Matter*, 2008, **20**, 184017-184039.

19. A. C. Basagiannis and X. E. Verykios, *Catal. Today*, 2007, **127**, 256-264.

20. A. C. Basagiannis and X. E. Verykios, *Appl. Catal., B*, 2008, **82**, 77-88.

21. I. Balint, A. Miyazaki and K.-i. Aika, *J. Catal.*, 2002, **207**, 66-75.

22. Q. Dai, S. Bai, Z. Wang, X. Wang and G. Lu, *Appl. Catal., B*, 2012, **126**, 64-75.

23. J. Okal and M. Zawadzki, *Appl. Catal., B*, 2009, **89**, 22-32.

24. L. Ran, Z. Qin, Z. Wang, X. Wang and Q. Dai, *Catal. Commun.*, 2013, **37**, 5-8.

25. H. Huang, Q. Dai and X. Wang, *Appl. Catal., B*, 2014, **158-159**, 96-105.

26. L. Hu, Q. Peng and Y. Li, *J. Am. Chem. Soc.*, 2008, **130**, 16136-16137.

27. U. Zavyalova, P. Scholz and B. Ondruschka, *Appl. Catal., A*, 2007, **323**, 226-233.

28. Z. Zhu, G. Lu, Z. Zhang, Y. Guo, Y. Guo and Y. Wang, *ACS Catal.*, 2013, **3**, 1154-1164.

29. A. V. Salker and M. S. F. Desai, *Appl. Surf. Sci.*, 2016, **389**, 344-353.

30. B. de Rivas, R. López-Fonseca, C. Jiménez-González and J. I. Gutiérrez-Ortiz, *Chem. Eng. J.*, 2012, **184**, 184-192.

31. J. Panpranot, J. G. Goodwin Jr and A. Sayari, *Catal. Today*, 2002, **77**, 269-284.

32. T. L. Stuchinskaya, M. Musawir, E. F. Kozhevnikova and I. V. Kozhevnikov, *J. Catal.*, 2005, **231**, 41-47.

33. Q. Cai and J. Li, *Catal. Commun.*, 2008, **9**, 2003-2006.

34. M. A. Coronel-García, A. I. Reyes de la Torre, J. A. Melo-Banda, A. L. Martínez-Salazar, R. Silva Rodrigo, N. P. Díaz Zavala, B. Portales Martínez and J. M. Domínguez, *International Journal of Hydrogen Energy*, 2015, **40**, 17264-17271.

35. J.-Y. Park, Y.-J. Lee, P. R. Karandikar, K.-W. Jun, J. W. Bae and K.-S. Ha, *J. Mol. Catal. A: Chem.*, 2011, **344**, 153-160.

36. H. Duan, D. Xu, W. Li and H. Xu, *Catal. Lett.*, 2008, **124**, 318-323.

37. P. Singh and M. S. Hegde, *Chem. Mater.*, 2009, **21**, 3337-3345.

38. D. R. Rolison, P. L. Hagans, K. E. Swider and J. W. Long, *Langmuir*, 1999, **15**, 774-779.

39. J. Chen, W. Shi, S. Yang, H. Arandiyan and J. Li, *J. Phys. Chem. C*, 2011, **115**, 17400-17408.

40. Y. Wang, A.-P. Jia, M.-F. Luo and J.-Q. Lu, *Appl. Catal., B*, 2015, **165**, 477-486.

41. J. L. Gautier, E. Rios, M. Gracia, J. F. Marco and J. R. Gancedo, *Thin Solid Films*, 1997, **311**, 51-57.

42. T. Cai, H. Huang, W. Deng, Q. Dai, W. Liu and X. Wang, *Appl. Catal., B*, 2015, **166-167**, 393-405.

43. Z.-Y. Tian, P. H. Tchoua Ngamou, V. Vannier, K. Kohse-Höinghaus and N. Bahlawane, *Appl. Catal., B*, 2012, **117-118**, 125-134.

44. S. G. Christoskova, M. Stoyanova, M. Georgieva and D. Mehandjiev, *Mater. Chem. Phys.*, 1999, **60**, 39-43.

45. K. Ji, H. Dai, J. Deng, X. Li, Y. Wang, B. Gao, G. Bai and C. T. Au, *Appl. Catal., A*, 2012, **447–448**, 41-48.

46. T. Garcia, S. Agouram, J. F. Sánchez-Royo, R. Murillo, A. M. Mastral, A. Aranda, I. Vázquez, A. Dejoz and B. Solsona, *Appl. Catal., A*, 2010, **386**, 16-27.

47. B. de Rivas, N. Guillén-Hurtado, R. López-Fonseca, F. Coloma-Pascual, A. García-García, J. I. Gutiérrez-Ortiz and A. Bueno-López, *Appl. Catal., B*, 2012, **121–122**, 162-170.

48. C. Zhang, C. Wang, W. Hua, Y. Guo, G. Lu, S. Gil and A. Giroir-Fendler, *Appl. Catal., B*, 2016, **186**, 173-183.

49. C. Zhang, W. Hua, C. Wang, Y. Guo, Y. Guo, G. Lu, A. Baylet and A. Giroir-Fendler, *Appl. Catal., B*, 2013, **134–135**, 310-315.

50. Q. Dai, S. Bai, X. Wang and G. Lu, *Appl. Catal., B*, 2013, **129**, 580-588.

Graphical abstract and textual abstract
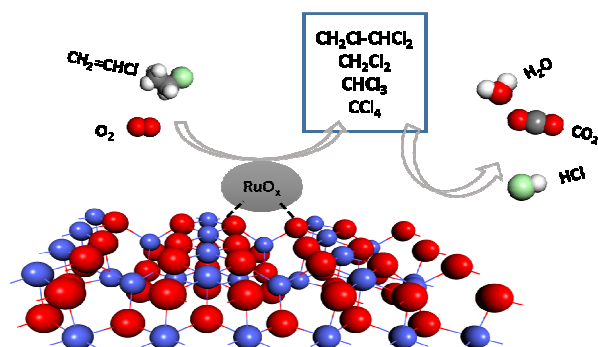
Ruthenium doped and supported cobalt oxides were prepared by sol-gel method and impregnation method. All the chlorinated intermediates were tracked during the oxidation process in temperature range. Oxygen vacancies and lattice oxygen mobility involved by Co^{2+} species and Ru^{4+} inpacted with Ru modification. The catalyst of 1%Ru/Co_3O_4 presented the best catalytic activity and stability for vinyl chloride oxidation, together with low concentration of chlorinated byproducts and high HCl selectivity.